United States Geological Survey Earthquake Hazards Program
Final Technical Report

USGS Award Number G17AP00026

Sparsity-based estimates of slow slip distributions in Cascadia

Author:

John Loveless

Department of Geosciences
Smith College
Clark Science Center
44 College Lane
Northampton, MA 01063, USA
Phone: (413) 585-2657
Fax: (413) 585-3786
Email: jloveles@smith.edu

Other personnel:

Elias Molitors Bergman, Smith College Post-baccalaureate Research Assistant
Sofia Johnson, Smith College Summer Undergraduate Research Fellow
Eileen Evans, United States Geological Survey Collaborator

Award Term:

January 1, 2017–December 31, 2017

ABSTRACT

Since the first geodetic detection of slow slip events (SSEs) on the Cascadia Subduction Zone in the 1990s, the role that these events play in the seismic moment balance of the plate boundary zone has been intensely studied. Slip during the events has been estimated to take place below the portion of the subduction zone that is inferred to be interseismically coupled and therefore most likely to generate future large earthquakes. However, the degree of spatial separation between the coupled and/or seismogenic zone, and the slowly slipping zone is ambiguous, in part because of the smoothing-based regularization technique that has been employed in many inversions of geodetic displacement fields for slow slip distributions. In this funded research, we compare two regularization strategies in estimating the distribution of slow slip: the classic smoothing-based approach and total variation regularization (TVR), which seeks spatial clusters of homogeneous slip, the magnitude of which may vary abruptly from patch to patch. Whereas smoothing inherently blurs the spatial distribution of estimated slow slip, and hence the degree to which that distribution may overlap with patterns of coupling and/or coseismic slip, TVR enables imaging of spatially distinct regions of slip behaviors. We find that TVR estimates of slow slip from a 20-year catalog of events are spatially correlated with the distribution of tremor and with a low degree of interseismic coupling. Our TVR-based estimates of slip suggest a segregation of the portions of the subduction zone that slip aseismically and those that are actively accumulating stress that may be released in future great earthquakes.

REPORT

Motivation

Slow slip events (SSEs) in Cascadia were first reported around 2000, following their recognition in continuous GPS position time series [Dragert et al., 2001]. Since then, numerous studies have examined the recurrence interval and along-strike variation thereof [Brudzinski and Allen, 2007], and collocation of these events with subduction zone coupling, earthquake slip, and non-volcanic tremor [Dragert et al., 2004; Wech et al., 2009]. Understanding the role that SSEs play in the moment budget of the subduction zone earthquake cycle is important: the aseismic slip serves to relieve accumulated stress, but its potential influence on the occurrence of ordinary earthquakes remains untested in Cascadia. Along the Mexico subduction zone, there is evidence that the 2016 M_W 7.3 Papanoa earthquake was triggered by a SSE that occurred immediately down dip [Radiguet et al., 2016]. This triggering process may have taken place because of the lack of spatial separation between the region estimated to have slipped aseismically and the coseismic rupture zone. In other subduction zones, however, there appears to be greater spatial distinction between the regions that slip slowly and the seismogenic zone [Gao and Wang, 2017]. Previous estimates of slow slip distributions [Szeliga et al., 2008] have used Laplacian smoothing to regularize the inversion of surface displacement for interface slip, and the inherent blurring of the slip distribution that arises from such regularization masks the possible separation between slow slipping regions and the interseismically coupled portion of the interface where great earthquakes may originate. Therefore, we seek an alternative means of regularizing the inversion

of displacement for slow slip distributions that allows the possibility of spatially and rheologically distinct regions that host the different slip behaviors.

Geodetic detection of slow slip events

We have generated a catalog of geodetic displacement fields for 31 slow slip events occurring since 1997 in the Oregon-Washington-Vancouver region the Cascadia subduction zone. We developed a slope (velocity)-based algorithm for detection of SSEs within geodetic position time series. This algorithm evaluates the long-term velocity over the duration of the time series, then uses a moving window to calculate average daily velocities over a ~3-week term. That is, for each day, we calculate a velocity for a 3-week span of daily position observations, first using the

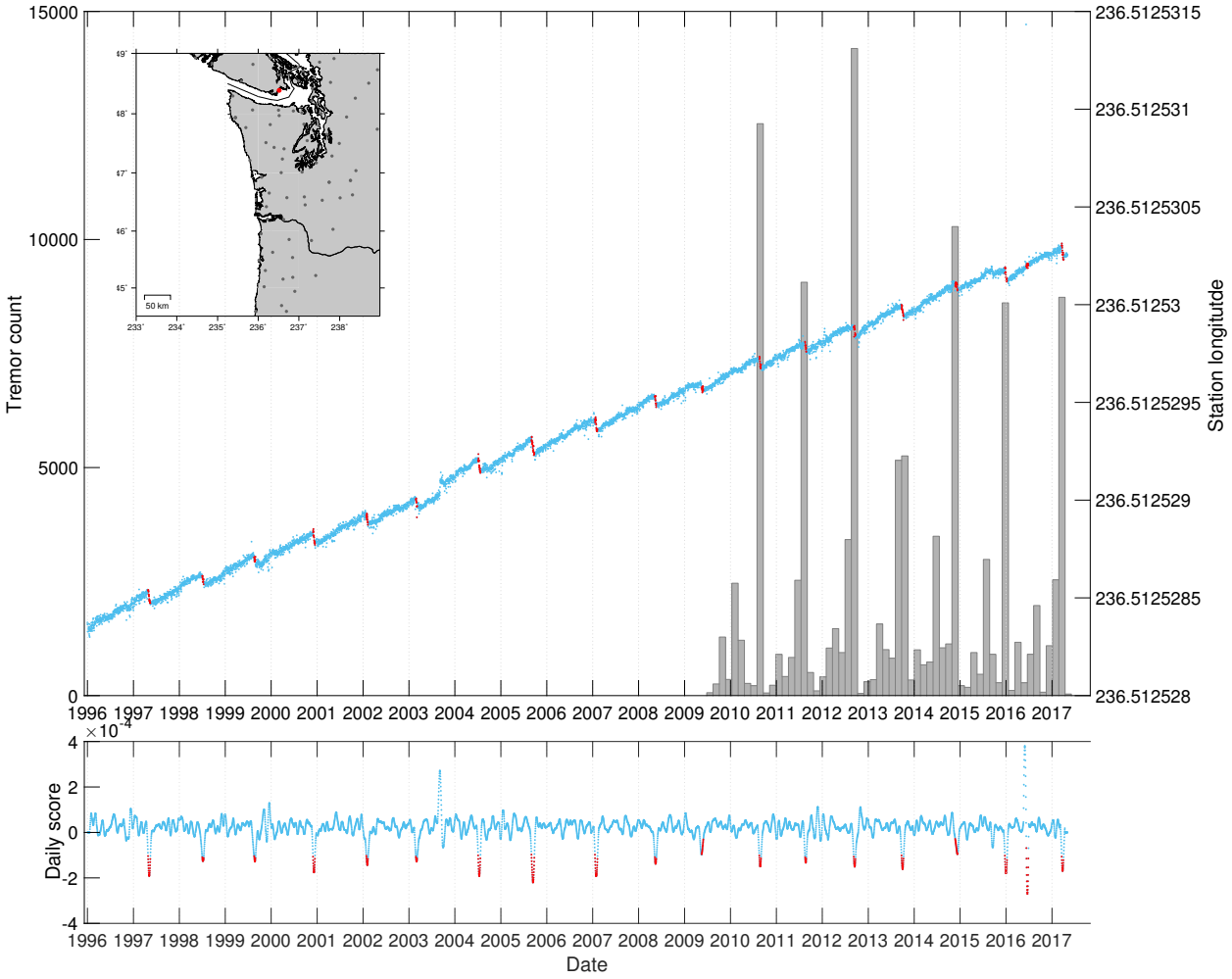

Figure 1. Detected slow slip events (SSEs) for station ALBH (shown in red on inset). Top: East component of daily position-time series from 1997-2017 (blue) with detected SSEs highlighted in red. Grey bars show 50 day bins of detected tremor epicenters within 1° of latitude of station. Spikes in number of tremor epicenters coincide with geodetically detected SSEs. Bottom: Results of slope comparison equation for daily positions. Negative excursions below a threshold (greater than six times the velocity calculated across the entire time series) are considered detected SSEs. The second to last detection was later removed by a filter, as the large positive and negative excursions are caused by single-day outlier position.

target day as the last of the observations, then the second-to-last, etc. until the target day is the first of the daily positions used for the velocity calculation. We then average these distinct velocity estimates and identify target days for which the average velocity deviates from the long-term velocity by a set factor, consistent with a reversal from nominally interseismic motion that is characteristic of SSEs [e.g., Dragert et al., 2001]. The net result is an overall score assigned to each day (Figure 1, bottom), corresponding to the likelihood that the station's movement on that day includes a contribution from a SSE. This score is similar to that generated by the algorithm of Crowell and Bock [2016], which was published at the time we were developing our own detection method.

The catalog of SSEs detected using our velocity-based algorithm is consistent with previous catalogs of events [e.g., Szeliga et al., 2008] and with non-volcanic tremor detected since 2009

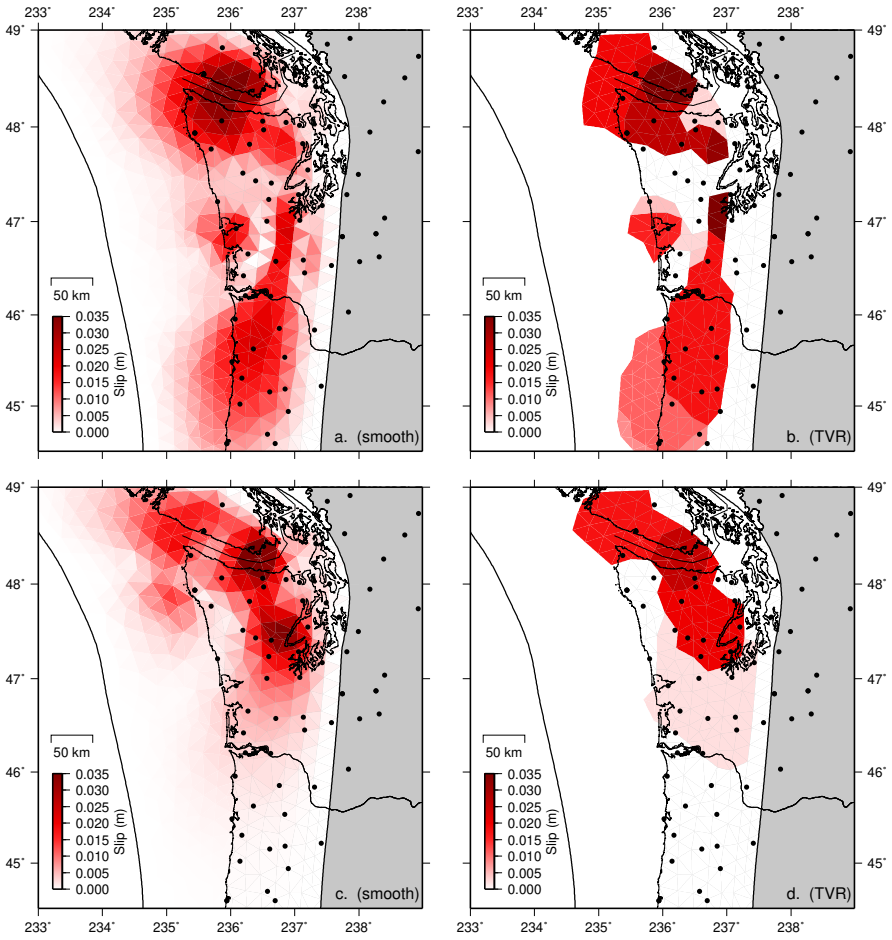

Figure 2. Comparison of estimated slow slip from smoothing-based and total variation regularization for two slow slip events. a. Smoothing-based slip distribution from the December, 2015 slow slip event. The mean residual surface displacement magnitude is 1.5 mm. b. TVR-based slip distribution from the same event, with a mean residual displacement of 1.3 mm. c. Smoothing-based and d. TVR-based estimates of slow slip during the March, 2017 event. As for the March, 2015 event, the fit to the constraining displacement fields is similar for both regularization methods (in this case, 2.3 mm for both).

[Pacific Northwest Seismic Network] in terms of the spatial and temporal distribution of events (Figure 1, top). We calculate displacement fields for each event by 1) linear least-squares fitting of each station's position time series from the starting to ending day of the event, 2) evaluating the function on the first and last days, and 3) taking the difference in these two positions. Displacement uncertainties are defined from the covariance of this least-squares fit.

Estimating slow slip distributions

Using the displacement fields determined from the detection algorithms, we estimate the distribution of slow slip taking place on the subduction zone interface, which we represent using triangular dislocation elements (TDEs) that mimic the geometry proposed by McCrory et al. [2006]. We estimate the slow slip distribution for each event using two different regularization schemes: Laplacian smoothing and Total Variation Regularization (TVR). Smoothing seeks to minimize the gradient of the slip magnitude between neighboring elements [e.g., Harris and Segall, 1987], whereas TVR promotes a sparse slip distribution, minimizing unique values of slip across the entire model geometry [e.g., Evans et al., 2015]. In general, the along-strike distribution of estimated slip is similar for all events between the two regularization schemes, but the down-dip extent is generally narrower and deeper in the TVR estimates than in those based on smoothing (Figure 2). Slip magnitudes are comparable between the two methods, as are geometric moments and misfits to the constraining geodetic displacements (Figure 2).

Comparison with other earthquake cycle slip processes

We compare the smooth and sharp estimates of cumulative slow slip distributions from 1997–2017 with patterns of interseismic coupling [Schmalzle et al., 2014] (Figure 3, left) and the spatial distribution of detected tremor since 2009 [Pacific Northwest Seismic Network] (Figure 3, right). In a region of the subduction zone near the northern Olympic Peninsula (Figure 3, inset), we find that the sharp up-dip limit of TVR-estimated slow slip at 20 km depth (green squares, Figure 3, right) coincides with that of tremor (gray polygon, Figure 3, right), and that the interface is interseismic coupled shallower than 20 km at ≥20% of the plate convergence rate (red dots, Figure 3, left). On the other hand, the more gradual up-dip decrease of smoothing-estimated slow slip (blue squares, Figure 3) substantially overlaps with the region of significant coupling and extends shallower than the up-dip limit of tremor distributions.

The abrupt up-dip termination of the cumulative slow slip estimated with TVR is consistent with the suggestion of Gao and Wang [2017] that there may be separation between portions of the interface that slip slowly and those capable of large-scale seismogenesis. Previous comparisons of cumulative slow slip estimated from geodetic displacement fields using smoothing-based regularization showed geodetically detected slip persisting farther up-dip than the tremor distribution [Wech et al., 2009]. By using a regularization technique that permits the spatial distribution of slip estimated from geodetic displacements to vary abruptly across the fault surface, we find better agreement between these two records of slow slip processes. Regardless of the regularization method, estimated slow slip distributions do show spatial overlap with partial coupling on the subduction interface [Schmalzle et al., 2014]. This is sensible, as the act of aseismic slip represents the release of some accumulated stress on the subduction interface. That said, we have developed preliminary TVR-based estimates of coupling, integrating the sparsity-promoting solver within the elastic block modeling framework of Meade and Loveless

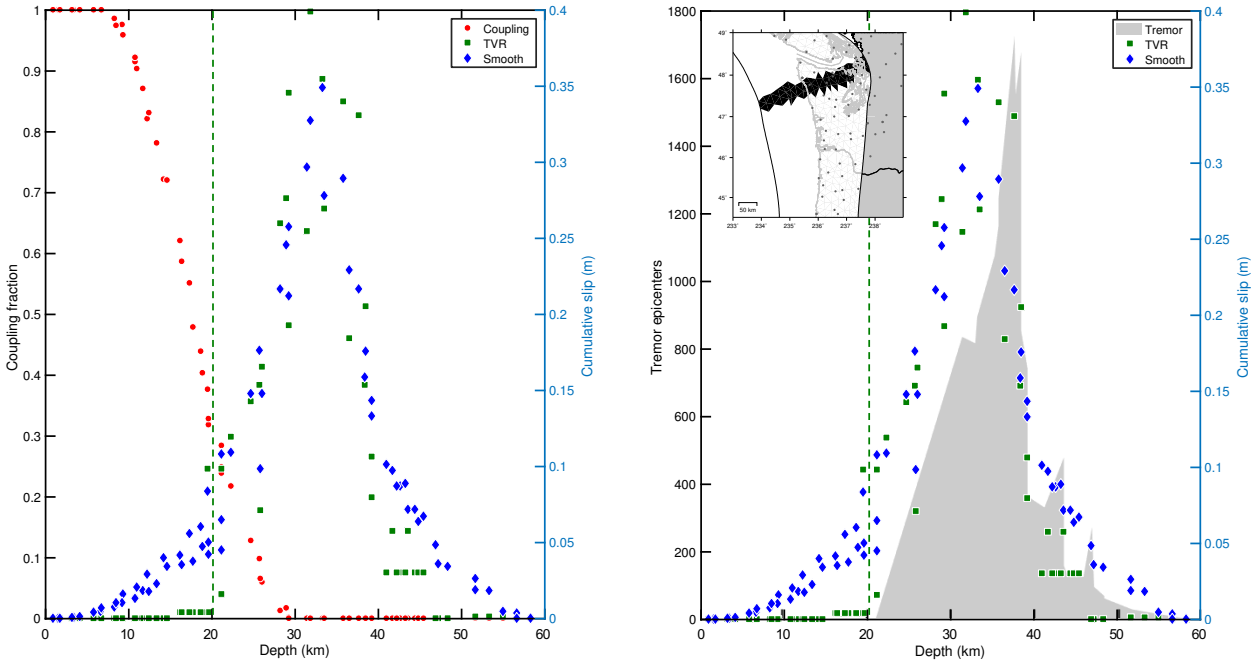

Figure 3. Depth profiles of estimated slow slip and other earthquake cycle slip processes. Left: Comparison of coupling magnitude (left axis, red squares) from Schmalzle et al. [2014] with our estimates of cumulative slow slip from 31 events spanning 1997–2017 (right axis). The green circles show slip magnitude estimated with total variation regularization (TVR) while the blue diamonds show slip estimated from the same displacement fields but with smoothing-based regularization. The dashed vertical line at 20 km depth marks the shallow truncation of TVR-estimated slow slip. Right: Comparison of cumulative tremor counts (2009–2017) [Pacific Northwest Seismic Network] as the filled gray region; green and blue symbols represent TVR and smoothing-based estimates of slow slip as in the left panel. Tremor is located deeper than 20 km, consistent with the slip estimated from geodetic displacements using TVR. Inset shows triangular elements of the parametrized subduction interface used in the coupling, slip, and tremor analysis.

[2009]. This work was supported by the present funding and a plan for its publication is in development.

Products of the funded research

Oral presentation at the 2017 AGU Fall Meeting, New Orleans, LA:

Molitors Bergman, E.G., E.L. Evans, and J.P. Loveless (2017), A 20-year catalog comparing smooth and sharp estimates of slow slip events in Cascadia, *EOS, Transactions AGU*, 98 (52), Fall Meeting Supplement, Abstract G42A-01.

Manuscript in preparation:

Molitors Bergman, E.G., E.L. Evans, and J.P. Loveless, A 20-year catalog comparing smooth and sharp estimates of slow slip events in Cascadia, in preparation for submission to *Journal of Geophysical Research*.

Geodetic time series analysis codes, displacement fields for all detected events, and estimated slip distributions for all events using both regularization schemes will be included as supplementary information upon publication.

References cited

Brudzinski, M. R., and R. M. Allen (2007), Segmentation in episodic tremor and slip all along Cascadia, Geology, 35(10), 907-910, doi: 10.1130/G23740A.1.

Crowell, B. W., Y. Bock, and Z. Liu (2016), Single-station automated detection of transient deformation in GPS time series with the relative strength index: A case study of Cascadian slow slip, Journal of Geophysical Research: Solid Earth, 121(12), 9077-9094, doi: 10.1002/2016JB013542.

Dragert, H., K. Wang, and T. S. James (2001), A silent slip event on the deeper Cascadia subduction interface, Science, 292(5521), 1525-1528, doi: 10.1126/science.1060152.

Dragert, H., K. Wang, and G. Rogers (2004), Geodetic and seismic signatures of episodic tremor and slip in the northern Cascadia subduction zone, EP&S, 56(12), 1143--1150.

Evans, E. L., J. P. Loveless, and B. J. Meade (2015), Total variation regularization of geodetically and geologically constrained block models for the Western United States, Geophysical Journal International, 202(2), 713-727, doi: 10.1093/gji/ggv164.

Gao, X., and K. Wang (2017), Rheological separation of the megathrust seismogenic zone and episodic tremor and slip, Nature, 543, 416, doi: 10.1038/nature21389.

Harris, R. A., and P. Segall (1987), Detection of a locked zone at depth on the Parkfield, California, segment of the San Andreas fault, Journal of Geophysical Research, 92(B8), 7945--7962.

McCrory, P. A., J. L. Blair, D. H. Oppenheimer, and S. R. Walter (2006), Depth to the Juan de Fuca slab beneath the Cascadia subduction margin: A 3-D model for sorting earthquakes, U.S. Geological Survey Data Series, 91(Version 1.2).

Meade, B. J., and J. P. Loveless (2009), Block modeling with connected fault network geometries and a linear elastic coupling estimator in spherical coordinates, Bulletin of the Seismological Society of America, 99(6), 3124-3139, doi: 10.1785/0120090088.

Radiguet, M., H. Perfettini, N. Cotte, A. Gualandi, B. Valette, V. Kostoglodov, T. Lhomme, A. Walpersdorf, E. Cabral Cano, and M. Campillo (2016), Triggering of the 2014 Mw7.3 Papanoa earthquake by a slow slip event in Guerrero, Mexico, Nature Geoscience, 9, 829, doi: 10.1038/ngeo2817 https://www.nature.com/articles/ngeo2817#supplementary-information.

Schmalzle, G. M., R. McCaffrey, and K. C. Creager (2014), Central Cascadia subduction zone creep, Geochemistry, Geophysics, Geosystems, 15(4), 1515--1532, doi: 10.1002/2013GC005172.

Szeliga, W., T. Melbourne, M. Santillan, and M. Miller (2008), GPS constraints on 34 slow slip events within the Cascadia subduction zone, 1997–2005, J. Geophys. Res., 113(B4), B04404, doi: 10.1029/2007JB004948.

Wech, A. G., K. C. Creager, and T. I. Melbourne (2009), Seismic and geodetic constraints on Cascadia slow slip, J. Geophys. Res., 114(B10), doi: 10.1029/2008JB006090.